# Water-level oscillations in the Adriatic Sea as coherent self-oscillations inferred by independent component analysis

**ARTICLE** *in* PROGRESS IN OCEANOGRAPHY · DECEMBER 2011

Impact Factor: 3.03 · DOI: 10.1016/j.pocean.2011.06.001



**4 AUTHORS:**

Paolo Capuano
Università degli Studi di Salerno


Enza De Lauro
Università degli Studi di Salerno


Salvatore de martino
Università degli Studi di Salerno


M. Falanga
Università degli Studi di Salerno

Progress in Oceanography 91 (2011) 447–460

Contents lists available at ScienceDirect

Progress in Oceanography

journal homepage: www.elsevier.com/locate/pocean

# Water-level oscillations in the Adriatic Sea as coherent self-oscillations inferred by independent component analysis

P. Capuano, E. De Lauro *, S. De Martino, M. Falanga

*Dipartimento di Ingegneria Industriale, Universitá degli Studi di Salerno, via Ponte Don Melillo, 84084 Fisciano (SA), Italy*

ARTICLE INFO

*Article history:*
Received 4 November 2010
Received in revised form 9 June 2011
Accepted 10 June 2011
Available online 24 June 2011

ABSTRACT

We analyze tide gauge records at four stations of the ISPRA network located in the Adriatic Sea basin (Eastern Italy), namely, going from North to South: Trieste, Ancona, Ortona and Otranto. We use linear and nonlinear methods in the frequency and time domains, including spectral and Independent Component Analysis (ICA), inter-times occurrence, and phase space embedding dimension evaluation. We show that four tidal constituents can be extracted by ICA and interpreted as coherent self-sustained oscillations. Finally, we show that these constituents can be reproduced by adopting a simple nonlinear oscillatory model that generalizes classical Andronov oscillator with the inclusion of a time dependent pumping.



## 1. Introduction

The dynamics of tides has often been considered akin to periodicity because of its origin rooted in the astronomical motion. Nevertheless, persistent irregularities of tides have been reported in the oceanographic literature over the years. In fact, evidence of this nonlinear behaviour, demonstrated experimentally at the end of the 1980s (Marchuk and Kagan, 1989), started to accumulate already at the beginning of the 20th century (Honda et al., 1908; Krummel, 1911). Consequently, simple nonlinear behaviours such as those associated with the production of self-sustained tones have already been partially explained in the description of tidal constituents (Maas, 1997).

At present, tides are described by using Navier–Stokes equations (Munk and Cartwright, 1966; Cartwright, 1977), that become nonlinear shallow water equations in a basin (see, e.g., Teo et al., 2003). The nonlinear effects are ascribed to a variety of factors that become relevant when tidal waves approach the coast and in the basins, i.e., at a given location, tides are affected by shallow water effects such as complex bathymetry, meteorological effects, wind, geometry of basins, bottom friction forces and so on.

Vittori (1992) studying water levels in the Venice Lagoon has shown that the irregularities of consecutive tidal maxima are related to low-dimensional chaos. More recent studies suggest that chaotic behaviours can be related to tidal motions also in the oceans (Maas and Doelman, 2002; Frison et al., 1999). These studies advocate the introduction of a fractal dimension phase space in order to obtain a full description of the asymptotic dynamics (Abarbanel, 1996).

One thus needs to reconcile the seemingly periodic behaviour of tides with the observed nonlinear effects.

The present paper fits in the line of thought that aims at understanding the tidal constituents in a basin as nonlinear, as first conjectured by Galileo in his controversial approach to the origin of tides (Palmieri, 1998; Galilei, 2001). Specifically, we analyse tides occurring in the Adriatic Sea basin (Eastern Italy) looking at experimental series consisting of water-level oscillations.

From the earliest studies, tides in the Adriatic Sea have been considered as a problem with one open boundary, whose solution is made particularly difficult by the complexity of flows due to the roughness of the coastline and bottom topography. Such complexities can be introduced in the shallow water equations as an advection and bottom friction term (Malačič et al., 2000). The ensuing linearized equations of motion incorporate the bottom topography as a suitable boundary condition. Some information about the main tidal constituents has been inferred by using the standard linear approach of the harmonic analysis (see, e.g., Melchior, 1978). However, even defining accurately the amplitudes and phases of different tidal constituents, either by integrating the linearized equations or by applying harmonic linear decomposition methods to the experimental data, the tides' predictability is not generally guaranteed because of their intrinsic nonlinearity.

In this paper, we search for the simplest solutions of the shallow water equations, which are self-sustained oscillations (i.e., a nonlinear system in a limit cycle regime) not by simulating the equations but rather by recovering the information from the experimental series. In doing so, we are faced with a typical inverse problem: we wish to extract from experimental data (the water

* Corresponding author.
*E-mail address:* edelauro@unisa.it (E. De Lauro).

0079-6611/$ - see front matter 
doi:10.1016/j.pocean.2011.06.001

level oscillations) the relevant information, including nonlinear features, on the fundamental constituents of the tides in a basin.

The concept of self-sustained oscillations was first formulated by Andronov (for a review, see, Andronov et al., 1966) in his theoretical investigation of radio-engineering devices. Self-sustained oscillations are oscillations maintained by the control induced by an even constant energy source. They describe a stationary regime, which follows a transient stage of excitation. A relevant feature of self-sustained oscillations is that their amplitude is stationary and does not depend on the initial conditions. In the general theory of dynamical system, self-sustained oscillations cannot be studied in the framework of a perturbative theory (Paul, 2007), as they are attractors for the dynamics.

According with the scheme sketched above, one should deal with the self-sustained oscillations of the Adriatic Sea and their relation to local tides in terms of synchronization, as expected in the framework of a nonlinear theory.

Synchronization is a mechanism of adjustment of rhythms in self-sustained oscillators due to their weak mutual interaction; this adjustment can be described in terms of phase locking and frequency entrainment. Synchronization phenomena have also been advocated in the description of collective coherent regimes in coupled systems (Rabinovich, 1974; Pikovsky et al., 2001; Capuano et al., 2009; De Lauro et al., 2009b).

After a pre-analysis in the frequency domain, in the following we will adopt techniques in the time domain, such as the Independent Component Analysis (ICA, hereafter), the inter-time occurrence, and the reconstruction of asymptotic dynamics. A time-domain approach (Jay and Kukulka, 2003) appears more appropriate in the investigation of nonlinear systems than the analyses based on the Fourier Transform, even though several tidal behaviours have been pointed out by frequency-domain methods.

## 2. Adriatic Sea

The Adriatic Sea is a long, narrow and semi-enclosed elongated basin separating the coast of Italy on the west side from the Balkan region on the eastern one. It is approximately 800 km long and 200 km wide and it is connected with the Mediterranean Sea through the Straits of Otranto in the southeastern part. It is divided into three sectors: the northern with an average depth less than 100 m; the central with depths in the range 100–250 m; the southern, instead, experiences an abyssal basin (South Adriatic Pit) whose depth exceeds 1300 m (see, e.g., Artegiani et al., 1997; Cushman-Roisin et al., 2001). The Italian coast is generally smooth with a single appendix, the Gulf of Trieste, at its north-eastern end. On the contrary, the Balkan coast, characterized by channels and islands, shows a very irregular topography (Tsimplis et al., 1995). Due to the basin characteristics, i.e., the low sea depth and the semi-closed shape, the tides in the northern Adriatic Sea have the highest amplitude over the whole Mediterranean Sea (Tsimplis et al., 1995). From the very beginning, tides in the Adriatic Sea have been interpreted as co-oscillations with Mediterranean and modeled considering a long semi-enclosed channel forced at the open end (Defant, 1961). In details, the diurnal surface tide has been interpreted in terms of near-resonant excitation of the fundamental Adriatic seiche by the Mediterranean tides, whereas the semidiurnal is the second mode co-oscillating (Mihanović et al., 2006). Recently, Cushman-Roisin and Naimie (2002) and Janeković et al. (2003) have shown that the direct astronomical forcing can explain only for a few percent of the observed amplitude, suggesting that the interplay with the Ionian Sea through the southern Adriatic boundary is a significant tidal driving force. On the basis of a suitable linearization of the Navier–Stokes equation, the dynamics of the tides in the Adriatic Sea have been simulated by using 2D models (for the northern sector) (Malačič et al., 2000) and 3D finite element free surface numerical model (for the whole basin) (Janeković et al., 2003). Specifically, the nature of the tides is reproduced by considering the superposition of seven main astronomical constituents (four semidiurnals and three diurnals), where the most energetic tidal constituents $M_2$, the semidiurnal component, and $K_1$, the diurnal one, have comparable amplitudes (Polli, 1959). Diurnals are addressed to topographic-gravity waves travelling from the eastern coastline to the western one, leading the shallow northern Adriatic at their right-hand side. Instead, semidiurnal tides are explained as a system of two Kelvin waves, propagating along the basis in opposite directions, leading to the amphidromic point between Ancona and Zadar, where the amplitude is expected to be very near zero, increasing towards north and south along the Adriatic Sea (Malačič et al., 2000). This approach surely allows to draw the co-tidal and co-range charts of tidal constituents as derived by means of harmonic analysis with an acceptable degree of accuracy. In this framework, the initial nonlinear partial differential equations (see, e.g., Lynch et al., 1996) are completely neglected. We remark that the quasi-periodic oscillations (i.e., limit cycle) must be solution of these equations (as firstly stated by Poincaré) and our attempt is to evidence the self-oscillating behaviour from experimental data.

## 3. Data set and spectral analysis

The data set studied in this paper has been acquired by the tide gauge network (RMN – Rete Mareografica Nazionale) managed by the National Agency for Environmental Protection and Technical Services (APAT), now a department of the Institute for the Environmental Protection and Research (ISPRA). This agency manages the real-time tidal gauge system, installed on several harbour inlets, located along the Italian coastline, including the islands. Each of these stations is equipped with an acoustic sensor that gauges and records the sea level electronically, with a sampling period of 10 min. Data are currently checked and validated according with the standard protocols. Station details can be found at http://www.mareografico.it.

We investigate the water-level oscillations collected at the tide gauges located in Trieste, Ancona, Ortona and Otranto, spanning the period from 16 March to 1 November 2006. The data are analyzed at the same temporal sampling of 10 min as they are acquired. Fig. 1a shows the Adriatic basin where the used tide gauge stations are indicated by a box. In the Adriatic, the harmonic approach identifies four major semidiurnal ($M_2$, $S_2$, $N_2$, $K_2$) and three major diurnal ($K_1$, $O_1$, $P_1$) constituents (Janeković and Kuzmić, 2005); cotidal charts of the main tidal constituents are reported in Fig. 1b (Lovato et al., 2010) The Rayleigh criterion for the separation of $S_2$ and $K_2$ frequencies demands a time series of 182.6 days. So, the duration of our record (230 days) is sufficient to completely resolve the principal tidal constituents.

We first determine the amplitude spectra (Fig. 2b) of the experimental series recorded at the selected four stations (Fig. 2a). As one can see, most significant constituents have periods corresponding to the diurnals and semidiurnals: the main peaks for the diurnals are 25.82 and 23.93 h, $O_1$ and $K_1$ in the standard harmonic description, whereas for the semidiurnals they are 12.42 and 12.00 h ($M_2$ and $S_2$); a remarkable low-frequency contribution and some higher frequencies are also evident. Specifically, the sea level $M_f$ tide is found to be a significant tidal constituent over periods between diurnal and semiannual (*SSA*) ones (Vilibic et al., 2010) whereas the high frequency portion of the spectrum contains ter-diurnal.

Energy involved in the tides is not regularly partitioned both among the stations and among the tidal constituents. In details,

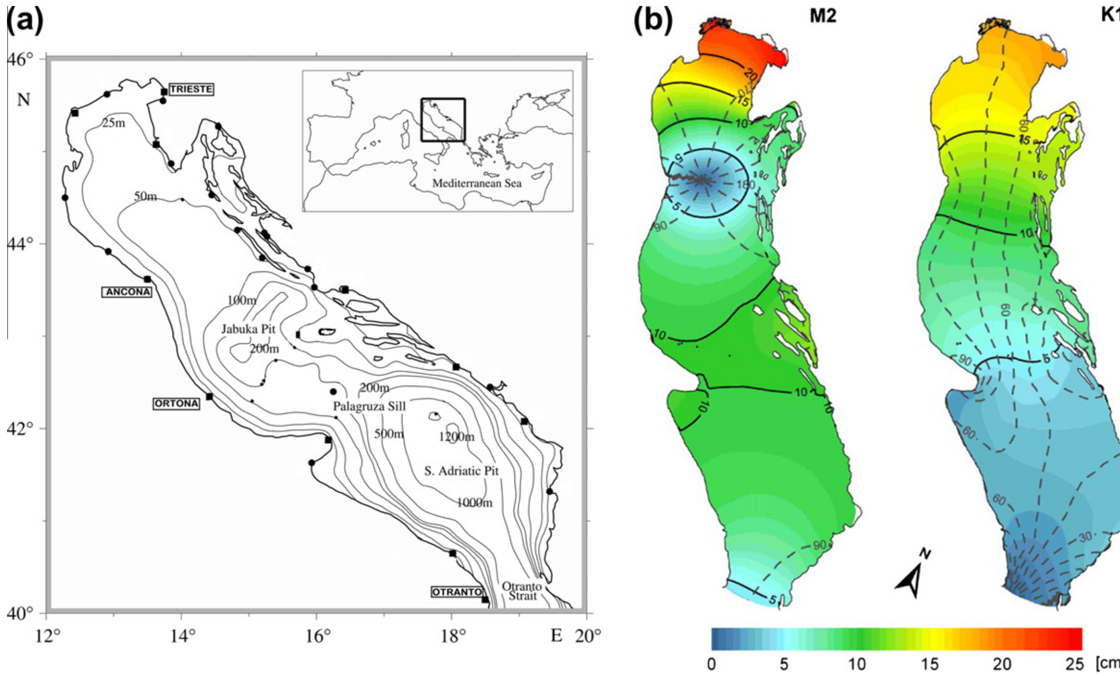


**Fig. 1.** (a) Location map of the tide gauge stations. The boxes surround the selected stations. (b) Co-tidal chart for $M_2$ and $K_1$ (from Lovato et al. (2010)).

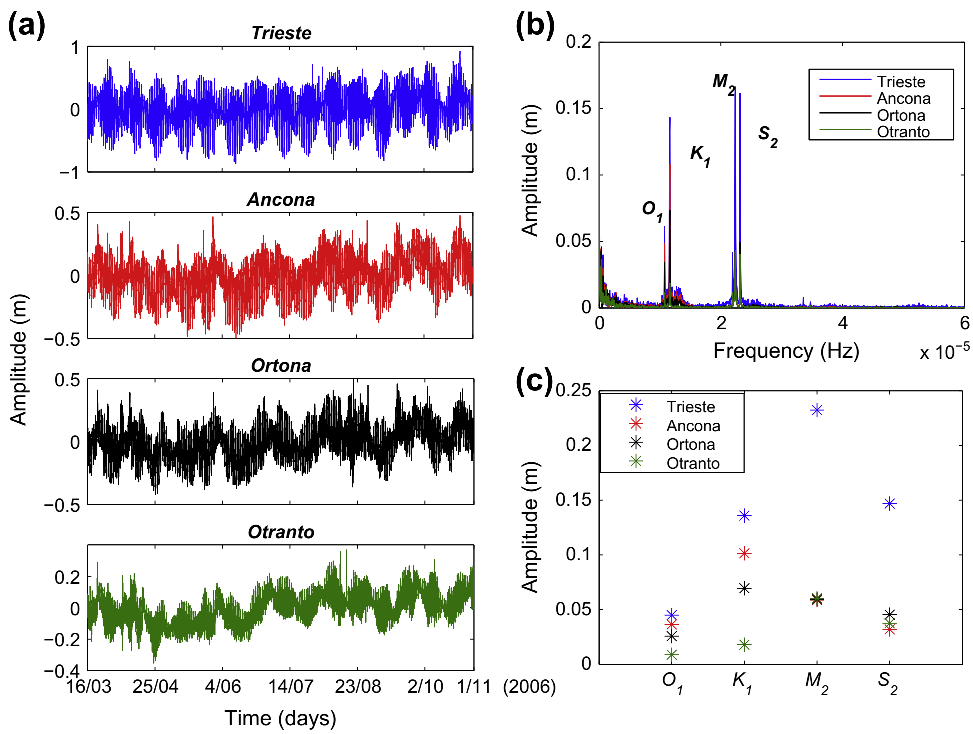


**Fig. 2.** (a) Water-level oscillations recorded at the four selected stations. (b) Superposition of the relative amplitude spectra. (c) Spectral amplitudes vs. tidal components for each station. The broadband spectra and the amplitudes depending on the frequency are an indication of the nonlinear effects in the water-level oscillations in the Adriatic basin.

the amplitude grows going from Otranto to Trieste where it is five times higher than Otranto (see Fig. 2a) according with the decreasing depth of the Adriatic basin and so with the influence of bottom friction. In addition, Otranto and Trieste are opposite in phase. Looking at the specific constituents, the amplitude of both $O_1$ and $K_1$ grows from Otranto to Trieste according with the enhancement in energy of the entire signals, whereas the semidiurnal components ($M_2$ and $S_2$) remain almost constant except for Trieste (see Fig. 2c). Moreover, $K_1$ is the fundamental mode for Ortona and Ancona, whereas $M_2$ is dominant for Otranto and Trieste. We remind the reader that Ancona is very close to the amphidromic point of semidiurnal tides.

This complex situation can also be enlightened by performing spectrogram analysis on series filtered in the range [1–40] h. In

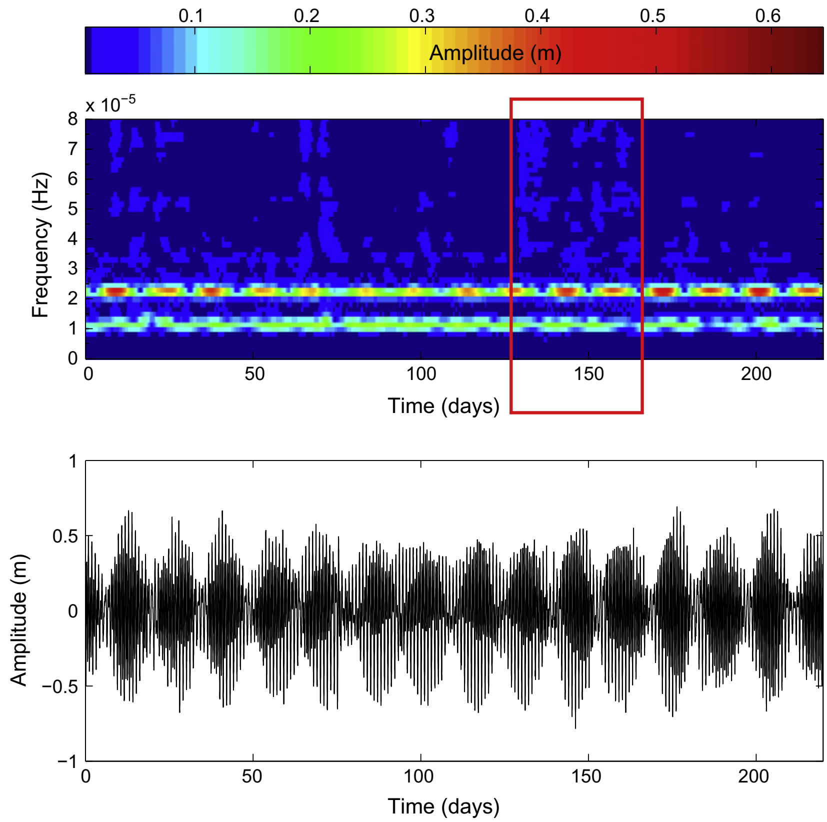


**Fig. 3.** An example of a spectrogram analysis performed on the sea level series recorded at Trieste from 2006/03/16 to 2006/11/01. We subdivide the series into 10 days long windows with an overlap of 90%. The vertical rectangle identifies a period with an enrichment of the high-frequency constituents.

Fig. 3, as an example, we report the results for the signal 230 days long and relative to Trieste. This plot clearly shows, besides the main periodicities, an enrichment in the higher frequencies (∼6 h) occurring in certain time periods (vertical red rectangle).[1] These results are independent of the considered station. These higher frequencies can be associated with self-oscillations of the Adriatic Sea assumed as a rectangular basin with a constant depth of 500 m and a length of 800 km.

Previous analysis indicates that energy distribution among the stations is unequal: this could be a symptom of nonlinearity in the physical system. It is worthwhile to remind that in any physical system a clear marker of nonlinearity is the frequency depending on amplitude. Therefore, we investigate how the relationship between amplitude and frequency changes in time. We look at the time evolution of the two dominant peaks and their relative amplitudes. Specifically, we compute frequency and relative amplitude by performing the spectrogram analysis on the entire signal within time windows 10 days long and overlapping for the 90% of their length (the best compromise between frequency resolution and fine time partitioning). Fig. 4d shows that, with respect to Otranto, over all time, the semidiurnal component retains the maximum content of energy and according with the amplitude variation it splits into two frequencies (traditionally, $M_2$ and $S_2$): on average the greater the amplitude the higher the frequency. Ancona and Ortona display an even more complex behaviour reported in Fig. 4b and c. At Ancona, the diurnal tides represent the dominant frequencies, but there are periods in which the semi-diurnals prevail. Considering that Ancona is very close to the amphidromic point of all semidiurnal constituents, it is interesting to extract periods in which semidiurnals prevail. This behaviour is more evident at Trieste, where there is an alternation of the two peaks (Fig. 4a). The relative importance of diurnal and semidiurnal tidal constituents as a function of time is better expressed evaluating the Form Number (defined as the ratio between the sum of $K_1$ and $O_1$ amplitudes and $M_2$ and $S_2$ ones) reported in Fig. 5 (Janeković and Kuzmić, 2005).

This characterization is enlightened in Fig. 6 in which the maximum spectral amplitude is shown in non-overlapping time windows (guaranteeing that no artificial correlations bias the dynamics). As can be seen, in Trieste and Ortona, there is a clear alternation between semidiurnal and diurnal peaks ruled by the ∼14-day tidal constituent as shown in Fig. 5. These characteristics were not evidenced in the spectral analysis and relate the lunar motion (half period) with the diurnal and semidiurnal ones.

The overall conclusion of this statistical analysis in frequency domain is that the system shows features of nonlinearity to be investigated in greater detail in a time-domain approach, which is more effective in retrieving nonlinearity.

## 4. Analyses in the time domain

In this section, we retrieve nonlinear features adopting time domain approaches, which appear more appropriate to study nonlinear systems. We note that there are physical systems with very similar Fourier transform but which are completely different in waveforms (see, e.g., De Lauro et al., 2005).

### 4.1. Independent component analysis: method

ICA is a method to find underlying factors or components from multivariate (multidimensional) statistical data, based on their sta-

[1] For interpretation of color in Figs. 1–5, 12 and 13, the reader is referred to the web version of this article.

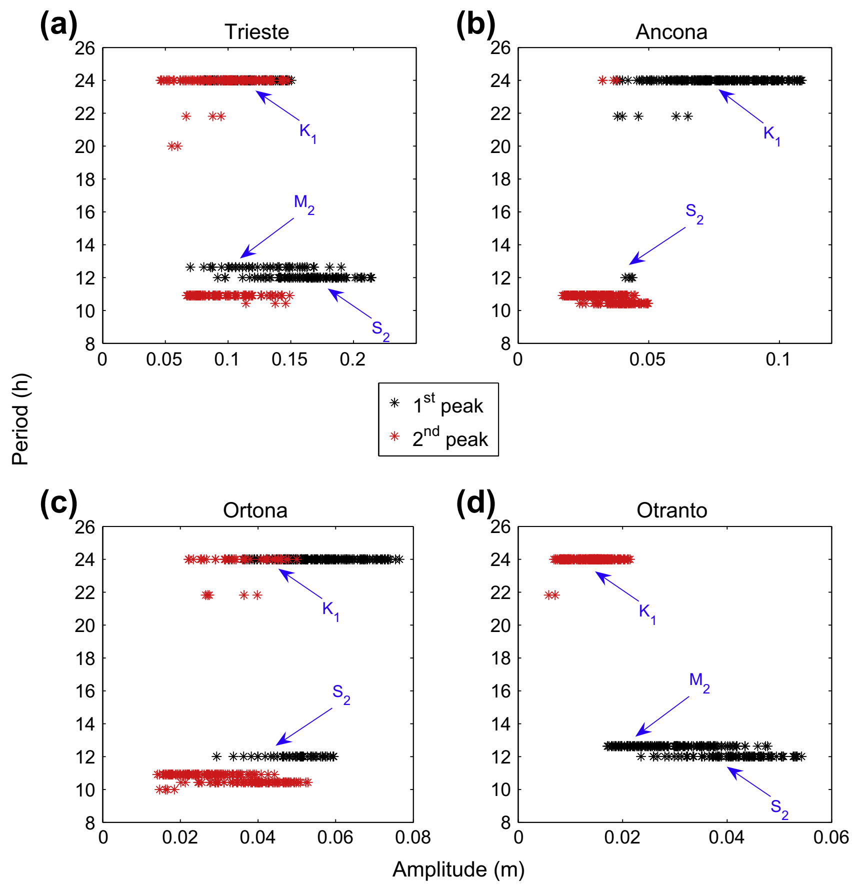


**Fig. 4.** The two predominant periodicities as a function of the heights for each station.

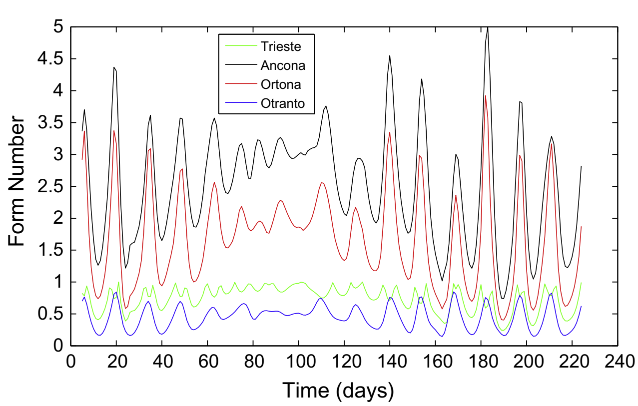


**Fig. 5.** The time behaviour of the Form Number evaluated for the selected period for the Adriatic Sea at each tide gauge. Spectral amplitudes have been evaluated in time windows 10 days long and overlapping for the 90%.

tistical independence (Hyvärinen et al., 2001). It has been introduced in the early 1980s by Hérault and Ans (1984) and developed for problems closely related to the cocktail party problem, namely the source separation problem related to the ability to focus one's listening attention on a single talker among a mixture of conversations and background noises. Several implementations of ICA can be found in literature but the algorithm, which has contributed to the application of ICA to a variety of problems for its easy implementation and mainly for its computational efficiency, was introduced by Hyvärinen and Oja (1997), i.e., the *fixed-point* FastICA algorithm. Since then, ICA has revealed many interesting applications in different fields of research (bio-medical signals, geophysics, audio signals, image processing, financial data, etc.). For instance, it was fruitfully applied to many natural systems as explosion-quakes and tremor at Stromboli and Erebus volcanoes (Acernese et al., 2003; Ciaramella et al., 2004b; De Lauro et al., 2008, 2009a), to study acoustical and mechanical vibrational field in organ pipe (De Lauro et al., 2007) or aerosol index in atmosphere (De Martino et al., 2002; Cuomo et al., 2009).

In its simplest form, ICA performs a blind separation of statistically independent components, assuming linear mixing of the components at the sensors. The components can be also nonlinear. The intuitive notion of maximum nongaussianity is used in ICA estimation adopting techniques which involve higher-order statistics; classical measures of nongaussianity are the kurtosis, the negentropy, and the mutual information.

We assume an instantaneous mixing model, thus neglecting any time delay that may occur in the mixing. Formally, the mixing model is written as

$$\mathbf{x} = \mathbf{A}\mathbf{s} \tag{1}$$

where $\mathbf{x}$ is an observed $m$-dimensional vector, $\mathbf{s}$ is a $n$-dimensional random vector to be estimated whose components are assumed to be mutually independent; $\mathbf{A}$ is a constant $m \times n$ matrix to be estimated.

The model can be recast in the following form:

$$\mathbf{x}_i = \sum_{j=1}^{n} a_{ij} s_j + v \tag{2}$$

An additive noise term $v$ is, generally, incorporated in the sum as one of the source signals. In addition to the independent assumption, we assume that the number of available different mix-

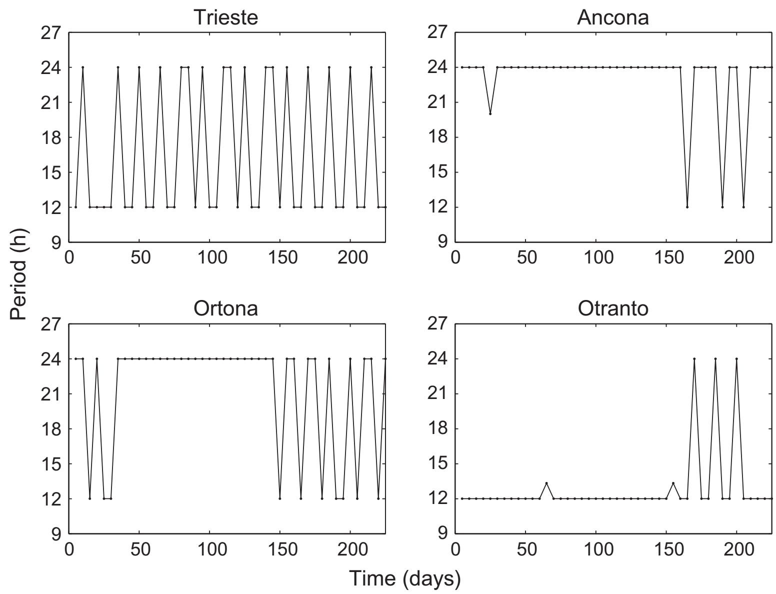


**Fig. 6.** Time evolution of the maximum spectral amplitude in non-overlapping time windows. The semilunar tide drives the principal constituent in Trieste, modulating the amplitude as visible in Fig. 5.

tures $m$ is at least as large as the number of sources $n$. Usually, $m$ is assumed to be known in advance, and often $m = n$ (there exists a probabilistic version of ICA that allows to by-pass this limit (Penny et al., 2001)). Only one of the source signals $s_i$ is allowed to have a Gaussian distribution, because it is impossible to separate two or more Gaussian sources (Bell and Sejnowski, 1995).

It is significant to underline that ICA is able to extract periodic signals from noise or nonlinear mixtures up to an amplitude ratio smaller than three order of magnitude. The technique is even more efficient in separating periodic signals (De Lauro et al., 2005).

#### 4.1.1. Pre-analysis: identification of tidal constituents through principal component analysis

Preliminarily, in order to reveal the internal structure of the data, i.e., to explain the variance in the data, we apply the Principal Component Analysis (PCA), which is an eigenvector-based multivariate analysis (Hyvärinen et al., 2001; Ciaramella et al., 2004a). In other words, imaging the water-level oscillations as a set of coordinates in a high-dimensional data space, PCA supplies the dimensionality of the data in as low as possible dimensional picture. Three significant eigenvalues emerge from this analysis (Fig. 7), suggesting a few degrees of freedom underlying the dynamical system. This result is in agreement with Capuano et al. (2009) who found that three degrees of freedom are necessary to describe the water-level oscillations in a global way by using methods of the reconstruction of the asymptotic dynamics.

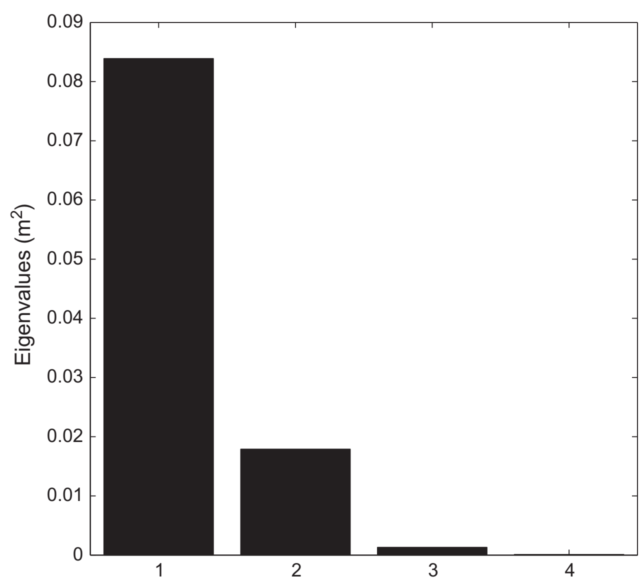


**Fig. 7.** Principal component analysis: three significant eigenvalues are extracted, suggesting a low-dimensional dynamical system.

#### 4.1.2. Application of ICA to the water-level oscillations

Once the dimensionality of the data is recognized, we apply ICA to our dataset in order to check whether a time decomposition is possible and to extract the amplitudes and waveform of the tidal constituents. We consider as input the recordings of the water-level oscillations acquired simultaneously at four stations.

In Fig. 8 the results of the application of ICA are reported. As can be seen, ICA decomposes data into four statistically independent components (the unknown sources **s** of Eq. (1)). Hereafter, the decomposition of the tides is no longer done in terms of harmonic tidal constituents ($M_2$, $K_1$, $S_2$, $K_2$) but in terms of ICs.

One can distinguish two independent components (IC1 and IC3) with main periods around semidiurnal and diurnal respectively. Each signal, resulting in a beat, is characterized by a main peak with adjacent peaks, which can no longer be separated even considering a wider data set made of eight tide-gauge time series.

In linear theory, these peaks are justified as being due to different sources. Nevertheless, there are physical systems, like the self-sustained musical instruments, where these beats can be interpreted as a splitting of the stable resonance of the air column in a thin-walled metal organ pipe. In fact, whenever a wall resonance frequency is close to that of the air column (Nederveen and Dalmont, 2004), instabilities occur and the air column oscillations switch between closely spaced frequencies. In other words, there are cases in which a unique source even constant might generate closely spaced frequencies without invoking broadband forcing or several sources.

Furthermore, ICA has identified a component (IC2) characterized by two main periods at 12.00 and 8.00 h. Looking at its wave-

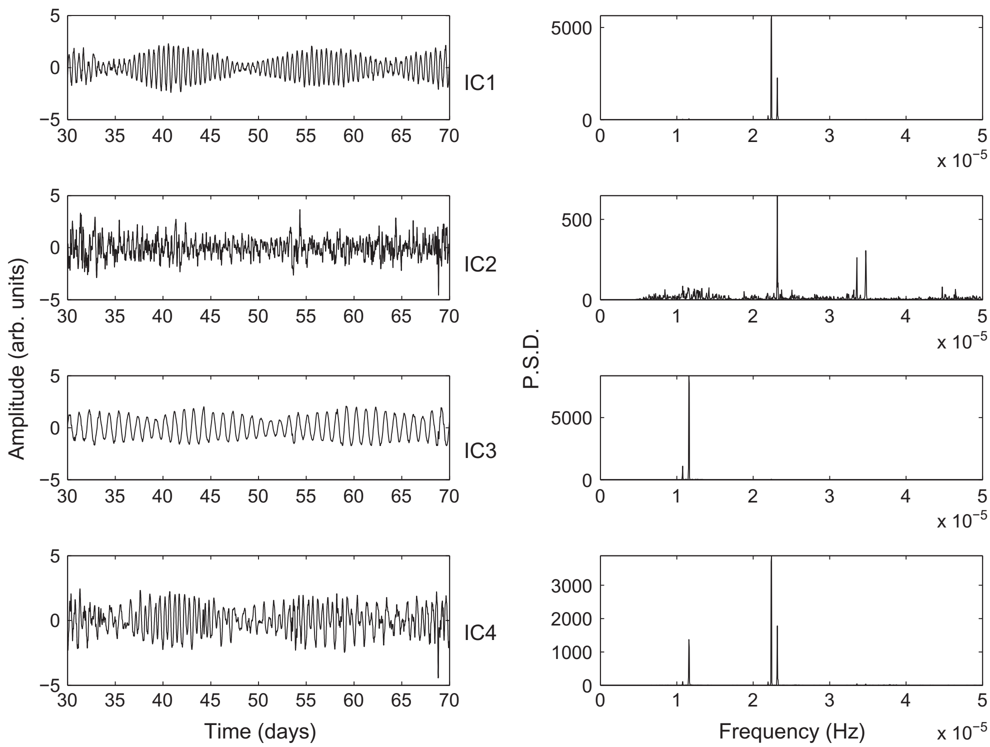


**Fig. 8.** Signals extracted by ICA with zero mean and unit variance: the first (IC1) shows a frequency content around the semidiurnal; the second (IC2) displays two main peaks around the semidiurnal and the ter-diurnal; the third (IC3) shows a frequency content around the diurnal; the fourth displays a waveform in which the diurnal and semidiurnal are intrinsically coupled.

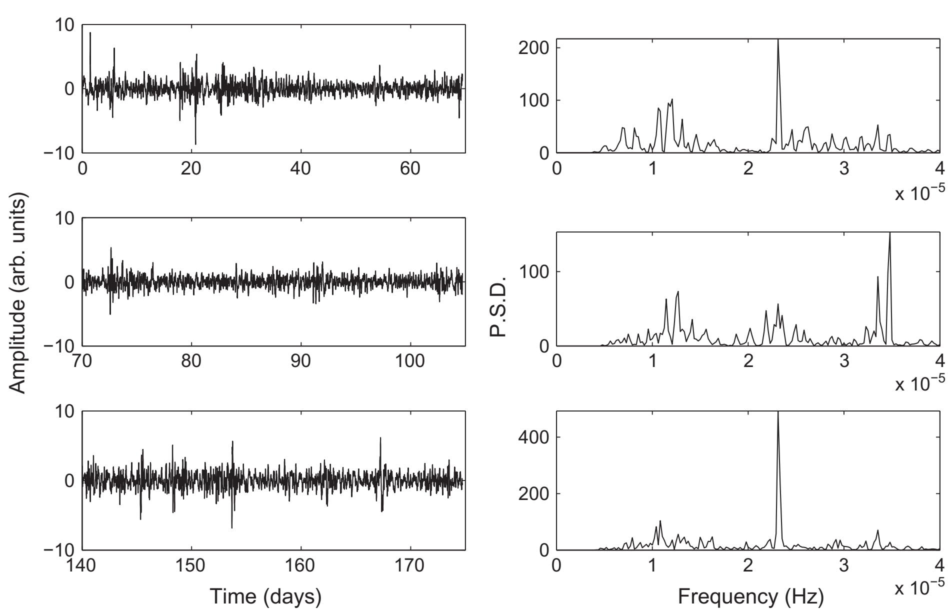


**Fig. 9.** The time evolution of IC2 puts in evidence the alternation of the two main peaks. In fact, the ter-diurnal appears dominant in the second panel.

form, one can observe that each peak becomes dominant in different periods. In fact, considering three non-overlapped time windows 69 days long, (Fig. 9) one can distinguish windows with a considerable frequency content around 12.00 h from others where the peak at 8.00 h is dominant.

The characteristics of IC2 might be related to some seasonal variation. We consider the evolution of a quantity proportional to the power of the main spectral peaks to investigate it in a more details. In Fig. 10 we report the power spectrum, estimated on the frequency bands as indicated by ICA in time windows 23 days long (starting from 16 March) to make a comparison with Fig. 9. We observe that the ter-diurnal is almost constant within the fluctuations and three orders of magnitude lower than the main constituents.

The fundamental (either diurnal or semidiurnal depending on the station) is modulated by means of both a lower periodicity related to the Moon's motion (lunar monthly or lunisolar fortnightly) and a seasonal variation. In particular, the latter reflects on the

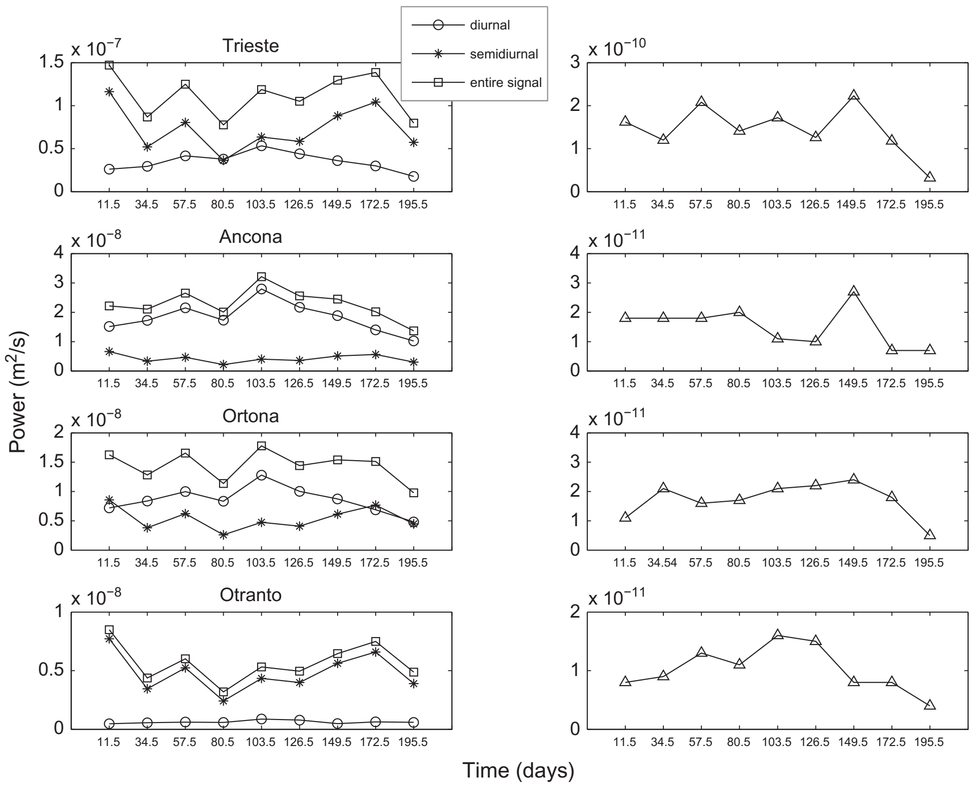


**Fig. 10.** Time evolution of a quantity proportional to the power of the main spectral peaks, estimated in time windows 23 days long. A lower periodicity related to the Moon's motion (lunar monthly for diurnal and lunisolar fortnightly for semidiurnal) and a seasonal variation modulate the tidal constituents.

semidiurnal, reducing its amplitude in summertime (see time windows 4–6, central part of Fig. 10). This reduction allows ICA to be able to extract the ter-diurnal. We note that ICA separates between nonlinear constituents if the amplitude ratio is lower than two orders of magnitude (De Lauro et al., 2005).

The last extracted component (IC4) displays diurnal and semidiurnal intrinsically coupled (Fig. 8).

### 4.1.3. Reconstruction of tidal elevations

After recovering the independent tidal constituents, the following step is finalized to retrieve their phases and amplitudes. This information is contained in the mixing matrix **A** estimated by means of ICA:

$$\mathbf{A} = \begin{pmatrix} -0.2038 & 0.0367 & -0.1688 & 0.0512 \\ -0.0337 & 0.0032 & -0.1152 & -0.0370 \\ 0.0595 & -0.0190 & -0.0741 & -0.0184 \\ 0.0583 & -0.0018 & -0.0170 & -0.0037 \end{pmatrix} \quad (3)$$

The mixing matrix reflects how the observed coherent oscillations are locally realized. The multiplication of **A** for the ICs gives the time domain waveform of the tides, hence recovering amplitude and phase.

Any extracted unitary-variance ICA source, multiplied for each coefficient of **A**, provides the waveform of a specific tidal component (including the proper phase and amplitude). In this way, we can construct a detailed tidal map at each site. Of course, since the dynamics is nonlinear, the amplitude of a single constituent can change as the measurement point changes. In Fig. 11, the independent components with proper amplitudes at all the stations are plotted.

The following step is to understand how the amplitude and phase (interpreted in terms of amplitude and waveforms in our scheme) of each independent component are related with the global dynamics. It is worthwhile to note that the semidiurnal components at Trieste and Ancona are in phase whereas they are opposite in phase with Otranto and Ortona (Fig. 12a). The component peaked at 12.00 and 8 h (IC2) displays the same behaviour (Fig. 12b). The diurnal contributions at all stations are in phase as shown in Fig. 12c. Finally, with respect to the IC4, only Trieste is opposite in phase to all the others (Fig. 12d).

Taking the mixing coefficient (A) multiplied by the maximum of the relative waveform as the representative amplitude of the IC tidal components, we can compare the heights (or at least the maximum expected value) of the tidal constituents at each location. This is shown in Fig. 13, where both IC3 and IC2 grow from Otranto to Trieste according with the enhancement in energy of the entire signals, whereas IC1 (semidiurnal component) remains almost constant except for Trieste where it represents the dominant peak.

It is important to note that the nonlinear analysis (ICA) has evidenced four components, one more than the linear analysis (PCA). It is worthwhile to underscore that superposition of these four components multiplied by mixing matrix elements reproduces the input signals at each station.

## 4.2. Intertime analysis

Further information on the nonlinearity of the water-level oscillations can be obtained by studying the inter-time occurrence between successive maxima in amplitude. In other words, we pick all the maxima greater than a certain threshold in sliding, non-overlapping time windows, and we calculate the distribution of time intervals (intertimes) between successive maxima.

Fig. 14 shows the time evolution of the intertimes (left panel), at fixed amplitude threshold, and time windows with relative histograms (right panel).

The functions of the intertimes show that the signals are not harmonic. Namely if one focuses attention on the diurnal and

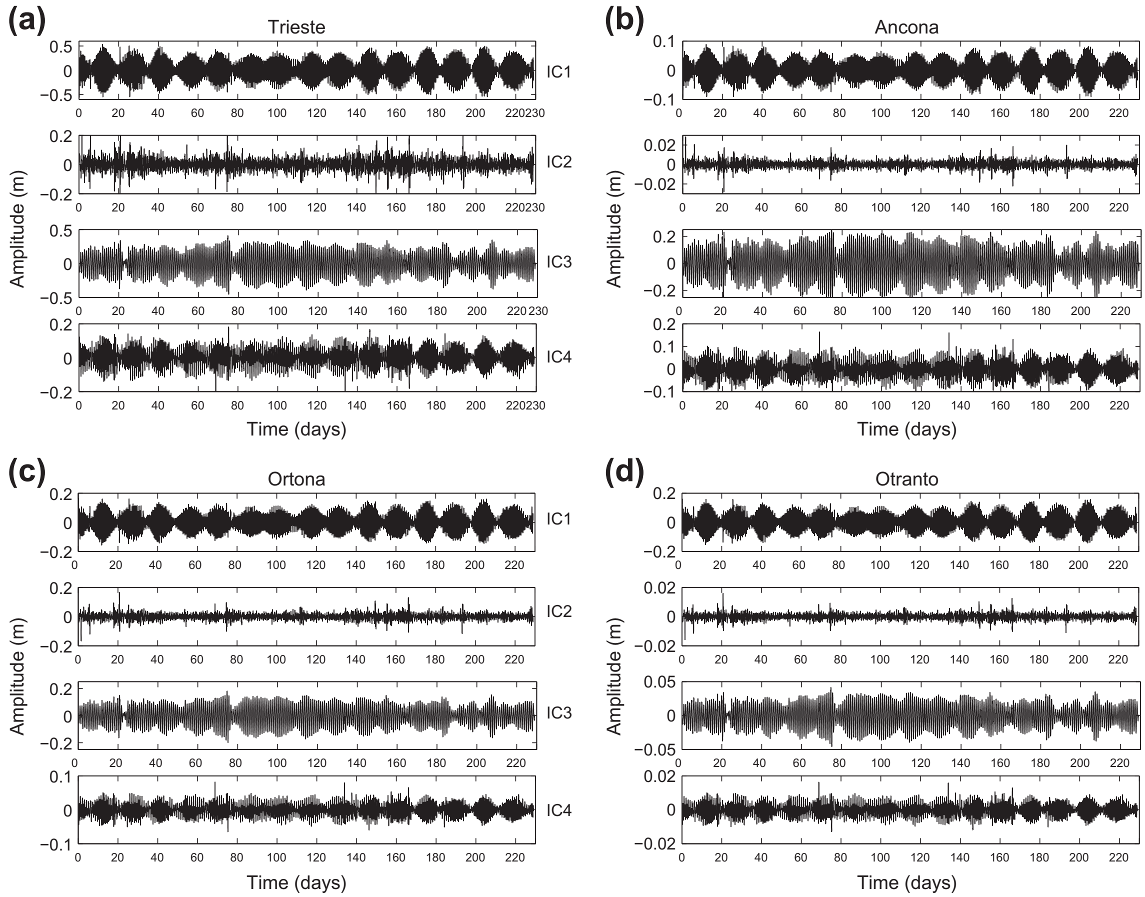


**Fig. 11.** Independent components with proper amplitudes for Trieste (a), Ancona (b), Ortona (c) and Otranto (d).

semidiurnal components, there exist several lines around each period suggesting quasi-periodic oscillations. A departure from periodicity can be quantified calculating the coefficient of variability, defined as the ratio between the standard deviation to the mean values of the intertimes (Cox and Lewis, 1966). This coefficient is zero for a periodic process and is one for a Poisson process.

Our distributions are Gaussian-like and they are characterized by coefficients of variability at least two orders of magnitude greater than an harmonic signal. For example, with respect to Trieste, fixing a threshold in amplitude at 0.03 m and a time window 20 min long, the variability coefficients are 0.15 and 0.08 for the semidiurnal and diurnal component respectively.

### 4.3. Reconstruction of the low-dimensional dynamic system

Reproducing the tides at a place generally requires numerical integration of the Navier–Stokes equations subject to complex boundary conditions. This is extremely difficult both for the intrinsic nonlinearity of the Navier–Stokes and for the lack of a detailed knowledge about the boundary conditions. Actually, we can approach the problem in a completely different way, just by observing that the simplest solutions of the full nonlinear Navier–Stokes equations are self-sustained oscillations. In that case, the infinite degrees of freedom of the tidal field (which should be derived by a complete solution of the equations) globally organize in a sort of a collective behaviour and tides can be described by a low dimensional dynamical system. Following this line of thought, in the framework of the theory of the dynamical systems, we explore the phase space in order to extract information about the effective degrees of freedom of the dynamics.

A standard procedure to reconstruct the asymptotic time evolution is the use of the time delay method. This method relies on the mathematical formulation due to Takens (1981) and it is extensively treated in the literature (see, e.g., Abarbanel, 1996). We select the Averaged Mutual Information (AMI) (Fraser and Swinney, 1986) and the False Nearest Neighbours (FNN) (Kennel et al., 1992) methods to calculate respectively the time delay and the dimension of the phase space whereby the dynamics evolves (embedding dimension). This dimension is an upper bound for the attractor dimension obtained by using the standard technique of Grassberger and Procaccia (1983) based on the correlation integral.

### 4.4. Results

Fig. 15 illustrates the application of FNN to the unfiltered water-level oscillations. The percentage of FNN is zero in correspondence of an embedding dimension of four (Fig. 15a). This means that a 4-dimension phase space is sufficient to fully unfold the dynamics. As an example, bi-dimensional projections of the four-dimensional reconstructed phase space relative to Otranto are reported in Fig. 16.

Finally, by applying Grassberger and Procaccia method to the raw signals, the existence of the plateau (Fig. 15b) suggests that the system is deterministic, nonlinear and establishes that the dynamics is low-dimensional with dimensions in the range [3–3.8]. This is in agreement with the results reported in Frison et al. (1999) for oceans.

A first study on the tidal data applying these methodologies was carried out by Vittori (1992) considering the Venice Lagoon. She

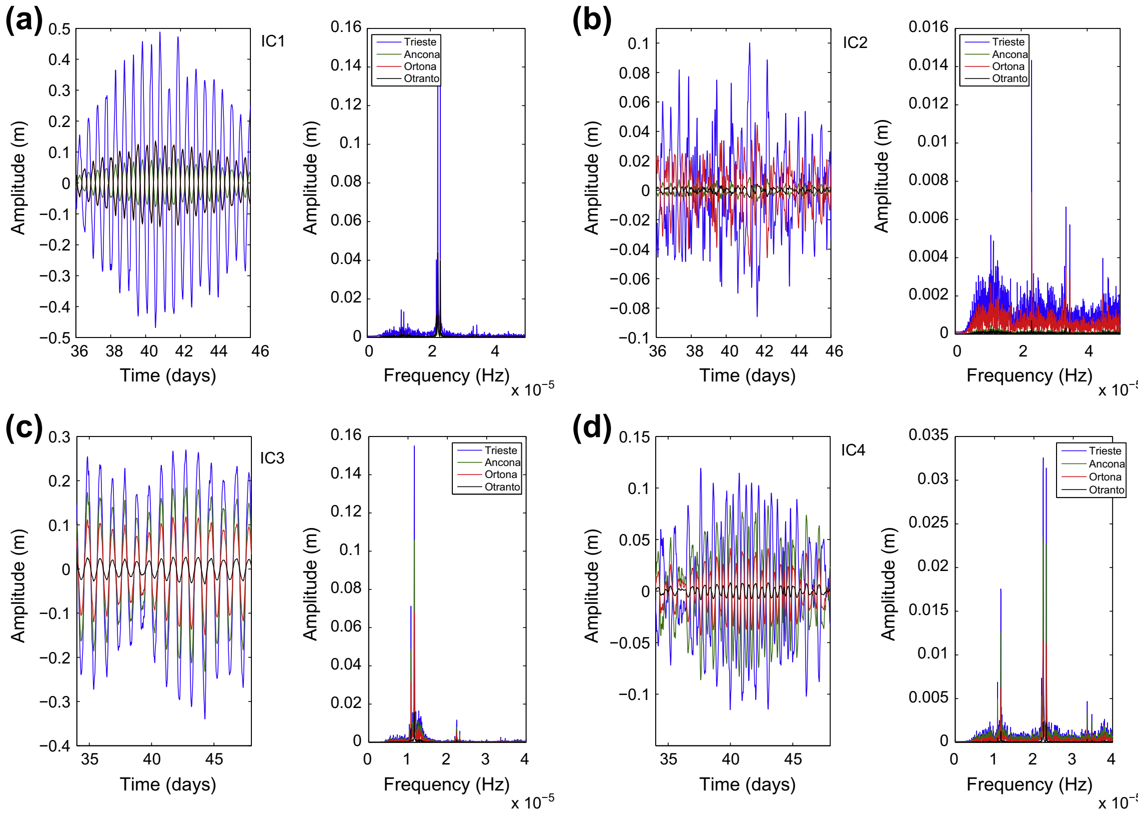


**Fig. 12.** Superposition of each independent component at the four stations.

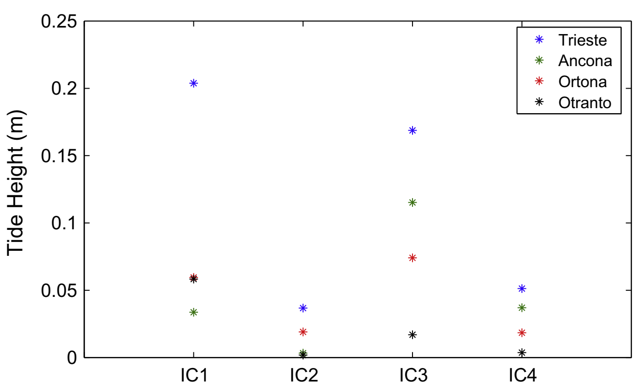


**Fig. 13.** Heights at Trieste, Ancona, Ortona, and Otranto for each ICA tidal constituent.

took advantage of the chaotic nature of the water level oscillations to make predictions of their time evolution.

## 5. An analogical model providing the tide signal

The nonlinearity (in the form of limit cycles) of the tides in the Adriatic Sea, evidenced in the previous sections, can also be supported by a simple nonlinear analogical model, which provides self-oscillations as solution. Before going into the details of the analogical model, it is worthwhile to summarize the main results. The water-level oscillations in the Adriatic Sea display:

1. self-sustained oscillations combined into broadband spectra;
2. amplitude-frequency dependence;
3. decomposition by ICA into four nonlinear components;
4. separation of the ter-diurnal related to the seasonal variations;
5. split lines for the intertimes and fractal embedding dimensions;
6. reconstruction of the heights of each tidal constituent from Otranto to Trieste related to the local characteristics of the basin.

The water-level oscillations at a point show many similarities with the vibrations of an organ pipe (Fabre and Hirschberg, 2000; Woodhouse, 1996): both fields are an effect of a globally organized phenomenon that appears in confined geometries due to a feedback mechanism. While the blowing pressure (energy source) in the organ pipe appears to be constant, the Adriatic water level oscillations display an energy source dependent on the time scales ranging from lunar cycles to seasonal variations. This last observation and item 3 suggest a non-trivial nonlinear oscillator as the basis for a complete tidal description; nevertheless, we can introduce a first approximate model, which reproduces one component at a point. This model contains the main aspects of the self-oscillations.

### 5.1. The Andronov oscillator

For our simulation we use the simplest dynamical system generating self-oscillations, i.e., the Andronov oscillator. It was first introduced to retrieve self-currents generated by a self-coupled triode: a triode is coupled with a RLC oscillator and an inductive feedback on the grid (Andronov et al., 1966). By neglecting the anode conductance, the grid currents and the inter-electrode capacitances, and assuming a piece-wise linear approximation for the valve characteristic $i_a = i_a(u)$, where $u$ is the grid voltage and $i_a$ is the anode current, simple equations can be derived:

$$LC\ddot{u} + RC\dot{u} + u = M\frac{di_a}{dt} \tag{4}$$

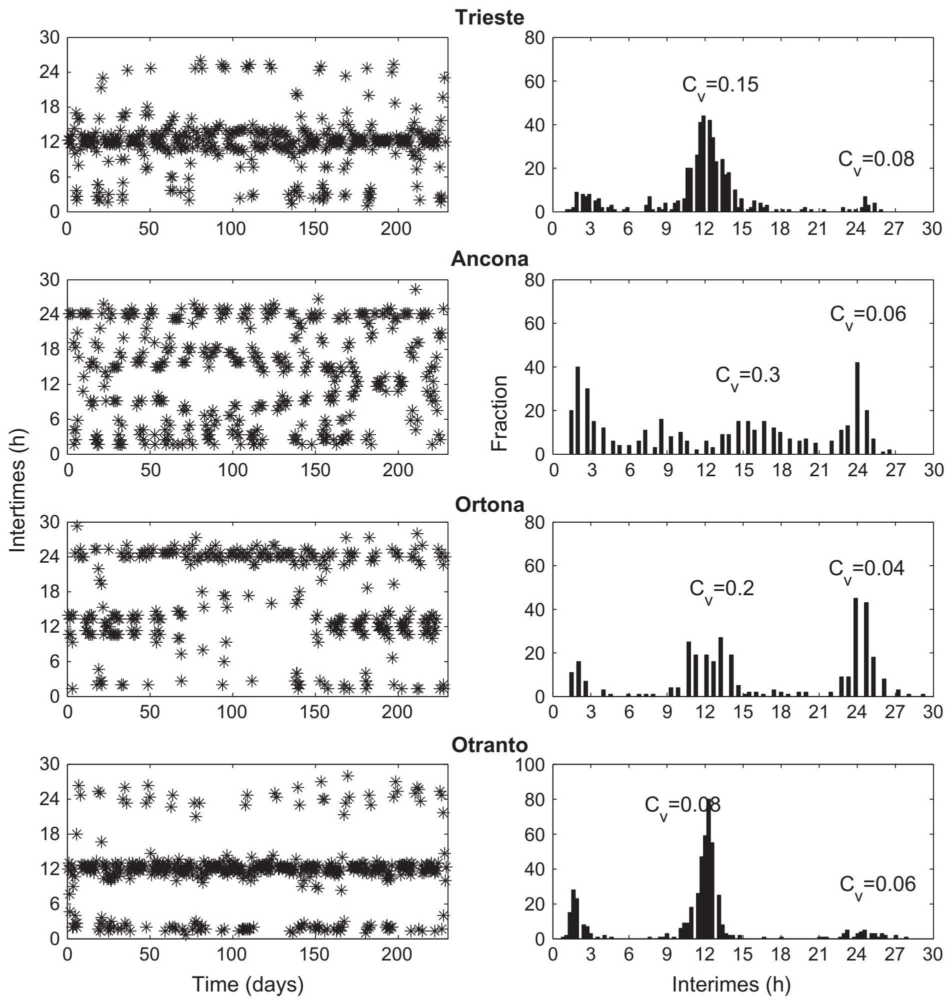


**Fig. 14.** Time evolution of the intertimes for the entire signal with respect to: (a) Trieste with threshold in amplitude at 0.03 m and time window 20 min long. (b) Ancona with threshold in amplitude at 0.05 m and time window 40 min long. (c) Ortona with no threshold in amplitude and time window 40 min long. (d) Otranto with threshold in amplitude at 0.03 m and time window 20 min long.

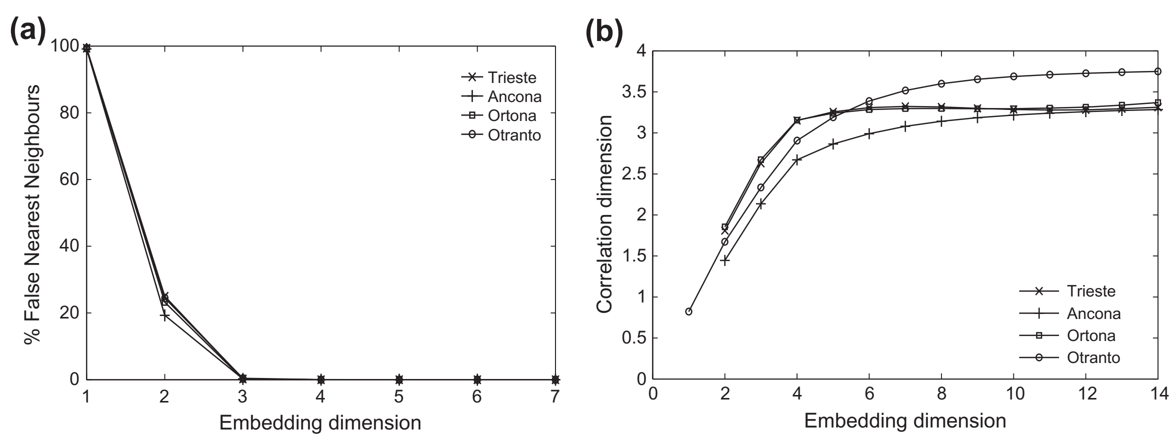


**Fig. 15.** Application of FNN to the water-level oscillations relative to all stations: (a) the fraction of FNN, as a function of the embedding dimension, goes to zero for embedding dimension equal to 4; (b) correlation dimension vs. the embedding dimension for the entire signal relative to all stations. As one can see, the plateau is stable around 3.6, suggesting that the system is low-dimensional.

$$i_a = f(u) = \begin{cases} 0 & u < -u_0 \\ S(u+u_0) & u > -u_0 \end{cases} \tag{5}$$

where $M$ is the mutual inductance (which has to be negative to install self-coupling); $S$ is the positive slope of the valve characteristic and $-u_0$ is the cut-off voltage. This system can be arranged in order to get the following very general equations:

$$\begin{aligned} &\ddot{x} + 2h_1\dot{x} + \omega_0^2 x = 0 \quad \text{for } x < b \\ &\ddot{x} - 2h_2\dot{x} + \omega_0^2 x = 0 \quad \text{for } x > b \end{aligned} \tag{6}$$

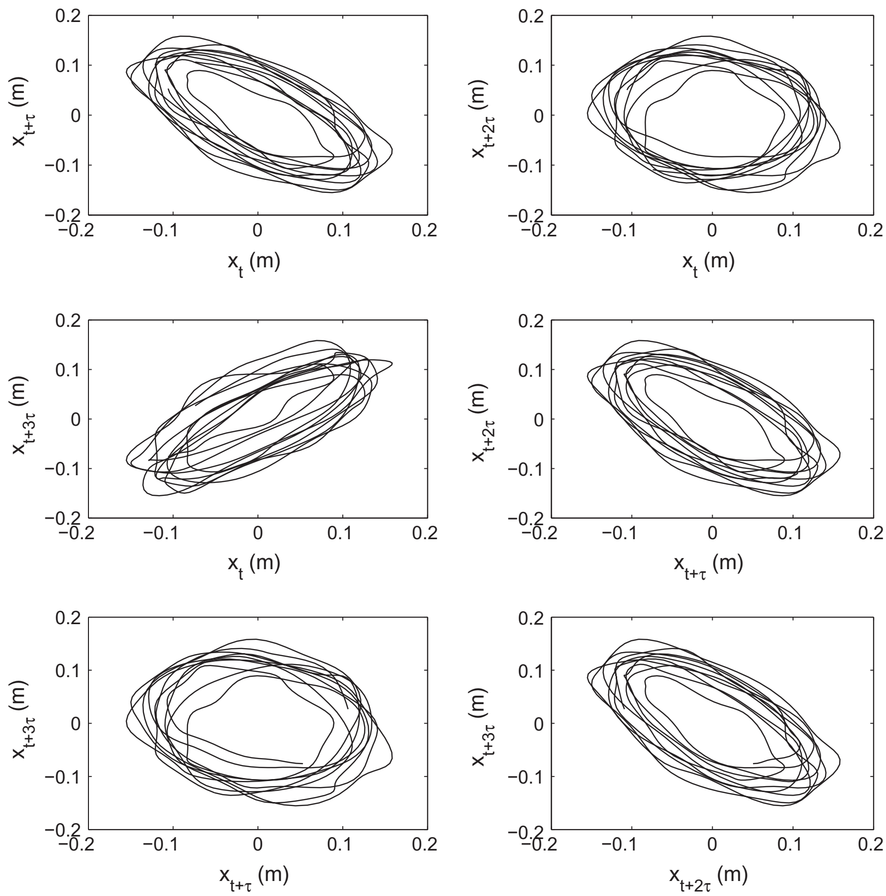


**Fig. 16.** Bi-dimensional projections of the four-dimensional reconstructed phase space relative to Otranto.

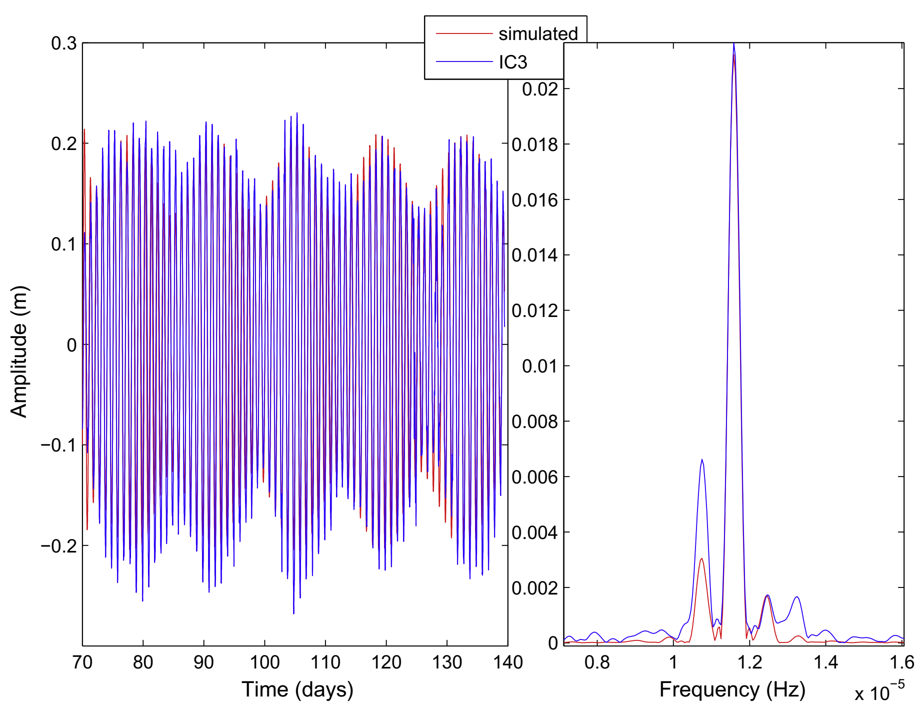


**Fig. 17.** Superposition of simulated signal and IC3. The parameters are $h_1 = 0.16,\ h_2 = 0.04,\ b = -0.1;\ T = \frac{2\pi}{\omega} = 23.9$ h, modulation at 27.3 days. The correlation coefficient is 0.9.

where $b$ is the hopping threshold in which the nonlinearity of the system is concentrated, $\omega_0^2 = \frac{1}{LC}$ is the natural frequency, $h_1 = \frac{\omega_0^2}{2}RC$ and $h_2 = \frac{\omega_0^2}{2}[MS - RC]$. The latter represent the dissipative and pumping parameters. The phase space is divided by a straight line $x = b$ into different regions identified by the two differential equations of the system. Notice that self-oscillations can be set up for suitable parameters and only if the threshold is negative (De Lauro et al., 2009b).

Apart from the derivation of this model based on electric circuits, formally the equations can hold for other systems, including basins, in which self-oscillations are settled by the competition of a dissipative and a pumping parameter. Specifically, $h_2$ and $h_1$ represent a pumping due to astronomical forcing and all the dissipative effects in a basin such as bottom friction.

Finally, in the linear case, before considering the extension to the continuum that produces the field equation (under a suitable limit), it is possible to describe the systems by a discrete approximation. We propose something similar with the Andronov oscillator as the fundamental brick.

### 5.2. Simulation of a diurnal component at a point

Since the main constituents are modulated by a seasonal variation, we restrict our analysis to a time window spanning from June to September (69 days long). In this period, the Adriatic Sea is working as an organ pipe (De Lauro et al., 2007) in which the proper modes are activated, i.e., 24, 12 and 8 h. As an example, we focus the attention on IC3 in Ancona reported in Fig. 11b (third panel from up). We note that the 24 h-tidal constituent is dominant here. To simulate this component we use the system of Eq. (6), introducing a pumping parameter dependent on time. To take into account the effects of lunar motion, as a first approximation, we let $h_2$ vary as a periodic function of 27.3 days. Its amplitude and the other parameters $b$ and $h_1$ are fixed by a best fit procedure. In Fig. 17 the comparison between IC3 and the simulation is shown. The waveforms are well correlated with a correlation coefficient equal to 95% and both the heights and the phases are well reproduced, including the close peaks in the spectrum.

## 6. Conclusion

We have analysed water-level oscillations recorded at four tide gauges along the Adriatic Sea. The different methodologies used both in the frequency and time domains, all show the existence of a nonlinear, self-oscillating behaviour. ICA identifies four nonlinear independent tidal constituents, which display differences from constituents obtained by harmonic analysis. Standard reconstruction procedures of the phase space embedding dimension result in low dimensional nonlinear dynamical systems, implying that only a few parameters are necessary to describe the tides at each point. In addition, the decomposition extracts time signals associated with the eigenfunctions that describe the tides. In particular, we note that the ter-diurnal component (which is always present) is extracted as an independent component only in specific periods, when the seasonal variation lowers the amplitudes of the diurnal and semi-diurnal constituents. We can summarize our findings as follows: in the Adriatic basin the water-level oscillations consist basically of four nonlinear tidal constituents (in the form of limit cycles) that are linearly superimposed. This implies that global and local aspects are, indeed, mixed together. Thus the classical resonance model advocated to describe tides in a basin appears inadequate.

Indeed, the ICA decomposition, the nonlinear relationship between the amplitudes and the frequency, and the shape of the spectrum (a main peak with smaller adjacent ones) remind us of the self-oscillations in musical instruments such as organ pipes (De Lauro et al., 2007). Proceeding with the analogy, the external astronomical forcing appears to act in the Adriatic Sea as the blowing pressure in an organ pipe, inducing the self-oscillation as the result of the interaction between the water and the basin. Therefore, it is possible to use a generalized self-oscillating Andronov system to simulate each extracted IC component. Specifically, introducing a pumping parameter in Eq. (6), depending on the lunar cycle, we have simulated the IC3 at Ancona. This model turns out to be sufficient to generate all the closely adjacent spectral peaks around the fundamental (the diurnal) reproducing all the complexity of the spectrum. We note that the estimated amplitude of pumping is numerically coincident with the inverse of the modulation periodicity and the estimated onset corresponds to the amplitude of 24 h as evaluated by the mixing matrix.

To simulate all the diurnals, we need only one nonlinear system rather than the three linear diurnal constituents as reported in several papers (see, e.g., Malačič et al., 2000). Moreover, this system providing self-sustained oscillations is an approximation of a suitable fluid equation. A general fluid dynamic model, built on this basis, could lead to a system of self-coupled equations involving also the vibration of the basin edges. This model requires more detailed analyses, looking at a dense network of tide gauges along the basin and also at other measurements beyond the water-level oscillations, such as the currents. Based on the experimental results, one may then introduce a forecast model (based on the Andronov oscillator) of tides without the needs of using complex grid models, since, locally, only a few degrees of freedom are involved in the dynamics.

## References


Abarbanel, H.D.I., 1996. Analysis of Observed Chaotic Data. Springer-Verlag, New York.

Acernese, F., Ciaramella, A., De Martino, S., De Rosa, R., Falanga, M., Tagliaferri, R., 2003. Neural networks for blind-source separation of Stromboli explosion quakes. IEEE Trans. Neural Netw. 14, 167–175.

Andronov, A.A., Vitt, A.A., Khaikin, S.E., 1966. Theory of Oscillators. Dover Publication, Inc., New York.

Artegiani, A., Bregant, D., Paschini, E., Pinardi, N., Raicich, F., Russo, A., 1997. The Adriatic Sea general circulation. Part I: Air–sea interactions water mass structure. J. Phys. Oceanogr. 27, 1492–1514.

Bell, A.J., Sejnowski, T.J., 1995. An information–maximisation approach to blind separation and blind deconvolution. Neural Computat. 7, 1129–1159.

Capuano, P., De Lauro, E., De Martino, S., Falanga, M., 2009. Analysis of water level oscillations by using methods of nonlinear dynamics. Int. J. Mod. Phys. B 23, 5530–5542. doi:10.1142/S0217979209063833.

Cartwright, D.E., 1977. Oceanic tides. Rep. Prog. Phys. 40, 665.

Ciaramella, A., Bongardo, C., Aller, H.D., Aller, M.F., De Zotti, G., Lähteenmaki, A., Longo, G., Milano, L., Tagliaferri, R., Teräsranta, H., Tornikoski, M., Urpo, S., 2004a. A multifrequency analysis of radio variability of blazars. Astron. Astrophys. J. 419, 485–500.

Ciaramella, A., De Lauro, E., De Martino, S., Di Lieto, B., Falanga, M., Tagliaferri, R., 2004b. Characterization of Strombolian events by using independent component analysis. Nonlinear Process. Geophys. 11 (4), 453–461.

Cox, D.R., Lewis, P.A., 1966. The Statistical Analysis of Series of Events. Metuen, London.

Cuomo, V., De Martino, S., Falanga, M., Mona, L., 2009. Influence of local dust source and stochastic fluctuations on Saharan aerosol index dynamics. Int. J. Mod. Phys. B 23, 5383–5390.

Cushman-Roisin, B., Gacic, M., Poulain, P.M., Artegiani, A. (Eds.), 2001. Physical Oceanography of the Adriatic Sea. Past, Present and Future. Academic Publ., Kluwer, p. 304.

Cushman-Roisin, B., Naimie, C.E., 2002. A 3D finite-element model of the Adriatic tides. J. Mar. Syst. 37, 279–297.

Defant, A., 1961. Physical Oceanography, vol. 2. Pergamon, Tarrytown (NY).

De Lauro, E., De Martino, S., Falanga, M., Ciaramella, A., Tagliaferri, R., 2005. Complexity of time series associated to dynamical systems inferred from independent component analysis. Phys. Rev. E 72 (1–14), 046712.

De Lauro, E., De Martino, S., Esposito, E., Falanga, M., Tomasini, E.P., 2007. Analogical model for mechanical vibrations in flue organ pipes inferred by independent component analysis. J. Acoust. Soc. Am. 122 (4), 2413–2424.

De Lauro, E., De Martino, S., Del Pezzo, E., Falanga, M., Palo, M., Scarpa, R., 2008. Model for high-frequency Strombolian tremor inferred by wavefield decomposition and reconstruction of asymptotic dynamics. J. Geophys. Res. 113, B02302. doi:10.1029/2006JB004838.

De Lauro, E., De Martino, S., Falanga, M., Palo, M., 2009a. Decomposition of high-frequency seismic wavefield of the Strombolian-like explosions at Erebus volcano by independent component analysis. Geophys. J. Int. 177, 1399–1406. doi:10.1111/j.1365-246X.2009.04157.x.

De Lauro, E., De Martino, S., Falanga, M., Ixaru, L.Gr., 2009b. Limit cycles in nonlinear excitation of clusters of classical oscillators. Comput. Phys. Commun. 180, 1832–1838. doi:10.1016/j.cpc.2009.05.005.

De Martino, S., Falanga, M., Mona, L., 2002. Stochastic resonance mechanism in aerosol index dynamics. Phys. Rev. Lett. 89, 12.

Fabre, B., Hirschberg, A., 2000. Physical modeling of flue instruments: a review of lumped models. Acta Acust. 86, 599–610.

Fraser, A.M., Swinney, H.L., 1986. Independent coordinates for strange attractors from mutual information. Phys. Rev. A 33, 1134–1139.

Frison, T.W., Abarbanel, H.D.I., Earle, M.D., Schultz, J.R., Scherer, W.D., 1999. Chaos and predictability in ocean water level measurements. J. Geophys. Rev. – Oceans 104 (C4), 7935–7951.

Galilei, G., 2001. In: Gould, S.J. (Ed.), Dialogue Concerning the Two Chief World Systems (S. Drake, Trans.). The Modern Library, New York.

Grassberger, P., Procaccia, I., 1983. Measuring the strangeness of strange attractors. Physica D 9, 189–208.

Hyvärinen, A., Oja, E., 1997. A fast fixed-point algorithm for independent component analysis. Neural Computat. 9 (7), 1483–1492.

Hyvärinen, A., Karhunen, J., Oja, E., 2001. Independent Component Analysis. John Wiley & Sons, New York.

Hérault, J., Ans, B., 1984. Réseaux de neurons á synapses modifiables: Décodage de messages sensoriels composites par une apprentisage non supervise et permanent. CR Acad. Sci. Paris III, 525–528.

Honda, K., Terada, T., Yoshida, Y., Isitani, D., 1908. Secondary undulations of oceanic tides. J. Coll. Sci. Tokyo 24, 1–113 (95 plates).

Janeković, I., Bobanović, J., Kuzmić, M., 2003. The Adriatic Sea $M_2$ and $K1$ tides by 3D model and data assimilation. Est. Coast. Shelf Sci. 57, 873–885.

Janeković, I., Kuzmić, M., 2005. Numerical simulation of the Adriatic Sea principal tidal constituents. Ann. Geophys. 23, 1–12.

Jay, D.A., Kukulka, T., 2003. Revising the paradigm of tidal analysis the uses of non-stationary data. Ocean Dynam. 53, 110–125.

Kennel, M.B., Brown, R., Abarbanel, H.D.I., 1992. Determining embedding dimension for phase space-reconstruction using a geometrical construction. Phys. Rev. A 45, 3403–3411.

Krummel, O., Handbuch der Ozeanographie, Verlag von J. Engelhorns Nachf. Stuttgart, 766, pp. 1911.

Lovato, T., Androsov, A., Romanenkov, D., Rubino, A., 2010. The tidal and wind induced hydrodynamics of the composite system Adriatic Sea/Lagoon of Venice. Cont. Shelf Res. 30, 692–706. doi:10.1016/j.csr.2010.01.005.

Lynch, D.R., Justin, T.C.I.P., Naimie, C.E., Werner, F.E., 1996. Comprehensive coastal circulation model with application to the Gulf of Maine. Cont. Shelf Res. 16, 875–906.

Maas, L.R.M., 1997. On the nonlinear Helmholtz response of almost-enclosed tidal basins with a sloping bottom. J. Fluid Mech. 349, 361–380.

Maas, L.R.M., Doelman, A., 2002. Chaotic tides. J. Phys. Oceanogr. 32, 870–890.

Malačič, V., Viezzoli, D., Cushman-Roisin, B., 2000. Tidal dynamics in the northern Adriatic Sea. J. Geophys. Res. 105, 26265–26280.

Marchuk, G.I., Kagan, B.A., 1989. Dynamics of Ocean Tides. Kluwer Academic Press, Dordrecht.

Melchior, P., 1978. The Tides of the Planet Earth. Pergamon, Paris, p. 609.

Mihanović, H., Orlić, M., Pasarić, Z., 2006. Diurnal internal tides detected in the Adriatic. Ann. Geophys. 24, 2773–2780. doi:10.5194/angeo-24-2773-2006.

Munk, W.H., Cartwright, D.E., 1966. Tidal spectroscopy and predication. Philos. Trans. Roy. Soc. Lond., Ser. A 259, 533–581.

Nederveen, C.J., Dalmont, J.P., 2004. Pitch and level changes in organ pipes due to wall resonances. J. Sound Vib. 271, 227–239.

Palmieri, P., 1998. Re-examining Galileo's Theory of Tides. Arch. History Exact Sci. 53, 223–375.

Paul, T., 2007. On the status of perturbation theory. Math. Struct. Comput. Sci. 17, 277–288.

Penny, [4] W., Roberts, S., Everson, R., 2001. In: Roberts, S., Everson, R. (Eds.), Independent Component Analysis: Principle and Practice. Cambridge University Press, Cambridge.

Pikovsky, A., Rosenblum, M., Kurths, J., 2001. Synchronization. A Universal Concept in Nonlinear Sciences. Cambridge University Press, Cambridge.

Polli, S., 1959. La propagazione delle maree nell'Adriatico, Atti del Convegno dell'associazione Geofisica Italiana, Roma, 111.

Rabinovich, M.I., 1974. Self-oscillations of distributed systems. Radiophys. Quant. Electron. 17, 361–385. doi:10.1007/BF01036796.

Takens, F., 1981. Detecting strange attractors in turbolence. In: Dynamical Systems and Turbolence Warwick. Lectures Notes in Mathematics, vol. 898. Springer, Berlin, pp. 366–381.

Teo, H.T., Jeng, D.S., Seymour, B.R., Barry, D.A., Li, L., 2003. A new analytical solution for water table fluctuations in coastal aquifers with sloping beaches. Adv. Water Resour. 26, 12391247. doi:10.1016/j.advwatres.2003.08.004.

Tsimplis, M.N., Proctor, R., Flather, R.A., 1995. A two dimensional tidal model for the Mediterranean Sea. J. Geophys. Res. 100, 16223–16239.

Vilibic, I., Sepic, J., Dadic, V., Mihanovic, H., 2010. Fortnightly oscillations observed in the Adriatic Sea. Ocean Dynam. 60, 57–63. doi:10.1007/s10236-009-0241-2.

Vittori, G., 1992. On the chaotic structure of tide elevation in the Lagoon of Venice. In: Proceedings of 23d International Conference on Coastal Engineering, Venice, Italy, American Society of Civil Engineers, pp. 1826–1839.

Woodhouse, J., 1996. Self-sustained musical oscillators. In: Mechanics of Musical Instruments. CISM Lecture Series. Springer-Verlag.